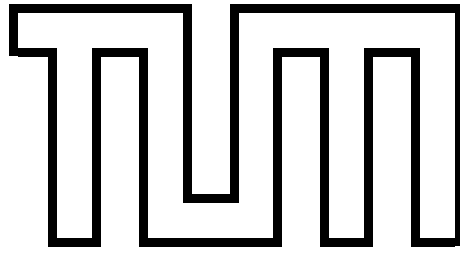# Technische Universität München

Department of Mathematics

Master's Thesis in Mathematics

Modelling and control of traffic flow on networks

Markus Stachl

Technische Universität München

Department of Mathematics

Master's Thesis in Mathematics

Modelling and control of traffic flow on networks

Modellierung und Kontrolle von Fahrzeugverkehr auf Netzwerken

Author:	Markus Stachl
Supervisor:	Prof. Dr. Massimo Fornasier
Advisor:	Dr. Giacomo Albi
Submission:	15.04.2017

I assure the single handed composition of this master's thesis only supported by declared resources.

München, 15.04.2017

(Markus Stachl)

Abstract

Zusammenfassung

Acknowledgements

Contents

Chapter 1

Introduction

1.1 Motivation

The goal of this thesis is...

1.2 Traffic flow modelling

Analyzing traffic flow has been an interdisciplinary research field of both mathematicians and civil engineers since the early 1950s. Over time different approaches for modelling traffic have been introduced and applied in extensive studies.

- On the **microscopic** scale every vehicle is considered as an individual agent whose dynamics are determined by the solution of an ordinary differential equation (ODE). The interaction between neighboring vehicles are usually based on simple equations and determine the behaviour of the collective. The most famous models of this approach are those of the *follow-the-leader* kind [21]. In those models the entire behaviour of the collective cars is fully determined by the one of the first car, namely the leader. Microscopic models can not only illustrate collective phenomena like traffic jams, but it can also be shown that under certain conditions the microscopic solution converges to the macroscopic solution as the number of vehicles approaches infinity [8].

- **Mesoscopic** - or kinetic - models analyze transportation elements in small homogenous groups, where the probability of each group to be at time t at location x with velocity v can be described by a function $f(t, x, v)$. The family of mesoscopic models includes headway distribution models [5] and cluster models [16]. This modelling approach often requires the use of methods from statistical mechanics.

- **Macroscopic** models utilize the similarities of traffic flow and fluid dynamics. In those models the change of averaged quantities, like density, velocity etc., is described by means of partial differential equations (PDE). The oldest representative

of macroscopic modelling are the LWR-models [22], named after their inventors M. J. Lighthill, G. B. Whitham and P. I. Richards. Others include the Aw-Rascle model and the Payne-Whitham approach [1, 20]. For the rest of this thesis, this is the modelling approach of choice.

In macroscopic models the target is to analyze the change of measurable quantities. A typical quantity used in the analysis of traffic flow, analogous to fluid dynamics, is the density of mass. Let us denote the traffic density on a space interval $[x_1, x_2]$ at some time $t \in \mathbb{R}$ as $\rho(x, t)$, then we can write the total mass on this interval as

$$\text{amount of cars} = \int_{x_1}^{x_2} \rho(x, t) dx \tag{1.2.1}$$

For conserved quantities no mass is neither destroyed nor created. Therefore the mass on an interval can only change by inflowing and outflowing quantities. The quantity mass crossing the point x at a time t is given by the **traffic flux** $f : [0, \rho_{max}] \rightarrow [0, f^{max}]$, where ρ_{max} denotes the maximum car density on the network.
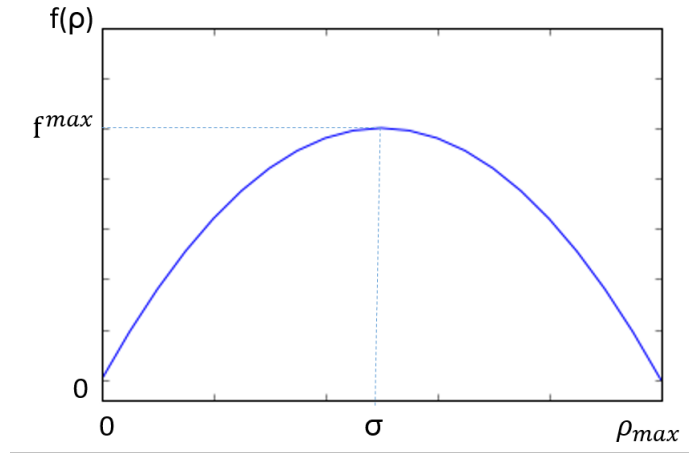
Figure 1.1: Typical shape of the fundamental diagram of traffic flow

The flux f, by assumption, is a Lipschitz continous function satisfying $f(0) = f(\rho_{max}) = 0$. We also assume that the traffic flux, or also referred to as *fundamental diagram*, follows the rule

$$f'(\rho)(\sigma - \rho) > 0$$

where

$$\sigma := \arg \max_{\rho} f(\rho) \tag{1.2.2}$$

denotes the density where the maximum flux

$$f^{max} := f(\sigma)$$

is attained. This value is usualy referred to as *road capacity*.

Since the total mass on the global space interval is preserved, the rate of change of the mass on the interval $[x_1, x_2]$ is defined by the difference of the in- and outfluxes of the interval (assuming that $\rho(x, \cdot) \in L^1_{loc}$, e.g.

$$\frac{d}{dt} \int_{x_1}^{x_2} \rho(x,t)dx \ = \ f(\rho(x_1,t)) - f(\rho(x_2,t))$$

Rewriting this assuming differentiability of both functions u and f and integration over the time interval $[t_1, t_2]$ leads to:

$$\int_{t_1}^{t_2} \int_{x_1}^{x_2} \frac{d}{dt}\rho(x,t) \ dxdt = \int_{t_1}^{t_2} \int_{x_1}^{x_2} \frac{d}{dx}\{-f(\rho)\} \ dxdt \tag{1.2.3}$$

Assuming that f is smooth, this leads the differential form of the **conservation law**:

$$\rho_t + (f(\rho))_x = 0 \tag{1.2.4}$$

The LWR-model, as it will be the basis for the remaining thesis, assumes that the flux $f(\rho) = \rho(x,t)v(x,t)$ is linearly dependent on the velocity $v(x,t)$ of the wave at point x. In particular the flux used for the LWR-model can be written as

$$f(\rho(x,t)) = \rho(x,t)v_{max}\left(1 - \frac{\rho(x,t)}{\rho_{max}}\right) \tag{1.2.5}$$

where u_{max} is the maximum density permitted by the road, and v_{max} the maximum velocity obtainable by the wave.

Other approaches like the Greenberg and Payne-Whitham model use highly nonlinear functions for their wave velocities, see [18, 20].

Extending the conservation law 1.2.4 with suitable initial conditions, we can formulate the full **Lighthill-Whitham-Richards model** as

$$\rho_t + \left[v_{max}\rho(1 - \frac{\rho}{\rho_{max}})\right]_x \ = \ 0 \qquad t > 0 \tag{1.2.6}$$
$$\rho(x,0) \ = \ \rho_0(x)$$

The remaining thesis will be structured as follows: In chapter 2 we will extend the given LWR-model on a network of roads in order to be able to analyze urban traffic situations. We will also introduce the concept of buffers to guarantee the existence of unique solutions for the model. In chapter 3 we will discuss the numerical procedures in order to qualitatively simulate traffic flow computationally. Chapter 4 will deal with introduce the concept of traffic lights on the network. We will then propose two different optimization methods to control the light signals in order to maximize the flux on the network. The two approaches consist of a rather brute-force approach and a concept called model predictive control (MPC). The thesis goes on with an expansion of the model by the concept of pollution in chapter 5 and ends with chapter 6 on future research.

Chapter 2

The LWR model on networks

So far we have only solved traffic flow problems on the real line. In order to analyze traffic flow more sophisticated problems under realistic scenarios, in particular in urban environments, it is necessary to extend the mathematical theory and the representation of traffic networks. The method of choice is hereby to represent traffic networks via directed graphs. This directed graph consists of a set of edges, representing the roads, and a set of nodes representing junctions. Every junction is thereby characterized by a finite number of incoming and a finite number of outgoing roads.

2.1 Related literature

Traffic flow on road networks has been a widely discussed topic over the past 70 years with an increasing intereenst in the past century.
 TODO:

- summary of cummulative number pde, multi-path, garavello approach...

A much larger and well presented genealogy of the history of traffic flow modelling can be found in [24].

2.2 Basic principles of networks

Rigorously we can define a network as followed, cf. [10]:

Definition 2.2.1 *A network is a tuple $(\mathcal{N}, \mathcal{E})$, where $\mathcal{N}$ is a finite collection of vertices, and $\mathcal{E}$ a finite collection of n_R edges, where every node represents a junction and every edge represents a unidirectional road. Each road $e_i = [a_i, b_i] \in \mathbb{R}, i = 1...n_R$ is defined over a real interval.*

We further require the following properties:

1) Every junction $J \in \mathcal{N}$ defines a union of two non-empty sets $\delta^{in}(J)$ and $\delta^{out}(J)$ where $\delta^{in}(J), \delta^{out}(J) \subset \mathcal{E}$, representing incoming and outgoing roads of the junction J, respectively.

2) For junctions $I, J \in \mathcal{N}, I \neq J$ we require $\delta^{in}(I) \cap \delta^{in}(J) = \emptyset$ and $\delta^{out}(I) \cap \delta^{out}(J) = \emptyset$

3) If $e_i \notin \bigcup_{J \in \mathcal{N}} \delta^{in}(J)$ then $b_i = \infty$. In this case $e_i \in \mathcal{E}^{out}$ where $\mathcal{E}^{out}$ denotes the set of all outgoing roads for the network. Furthermore if $e_i \notin \bigcup_{J \in \mathcal{N}} \delta^{out}(J)$ then $a_i = -\infty$. In this case $e_i \in \mathcal{E}^{in}$ where $\mathcal{E}^{in}$ denotes the set of all incoming roads for the network.

These assumptions guarantee that the resulting network is indeed a valid graph. Requirement 2) implies that every road starts and ends in at most one junction. Requirement 3) then says that if a road does not start (end) at a junction then it is considered as an inflow (outflow) of the network.

Another method to represent a road network is via so-called **adjacency matrices** [2].

Definition 2.2.2 *Let $\mathcal{N}$ be a set of edges with $|\mathcal{N}| = n_R$. Then the adjacency matrix A is a square $n_R \times n_R$-matrix with*

$$A_{ij} = \begin{cases} 1 & \text{if there exists a junction between road } e_j \text{ and } e_i \\ 0 & \text{else} \end{cases}$$

The adjacency matrix stores information if there is a direct connection between road e_j and e_i.

Remark:
The adjacency matrix only provides information about the general infrastructure of the network. Later on we will incorporate information about the drivers' turning preferences $\Theta_{i,j}$. We then speak of the transition matrix Θ with

$$\Theta_{ji} = \begin{cases} \Theta_{i,j} & \text{if there exists a junction between road } e_j \text{ and } e_i \\ 0 & \text{else} \end{cases}$$

where $\Theta_{i,j} \in [0, 1]$ reflects the preference of a driver coming from road e_i and leaving the junction in direction of road e_j.

Example 1 *Let us consider the network displayed in figure 2.1. Then the corresponding adjacency matrix can be written as*

$$A = \begin{pmatrix} 0 & 0 & 0 & 0 & 0 \\ 0 & 0 & 0 & 0 & 0 \\ 1 & 1 & 0 & 0 & 0 \\ 0 & 0 & 0 & 0 & 0 \\ 0 & 0 & 1 & 1 & 0 \end{pmatrix}$$
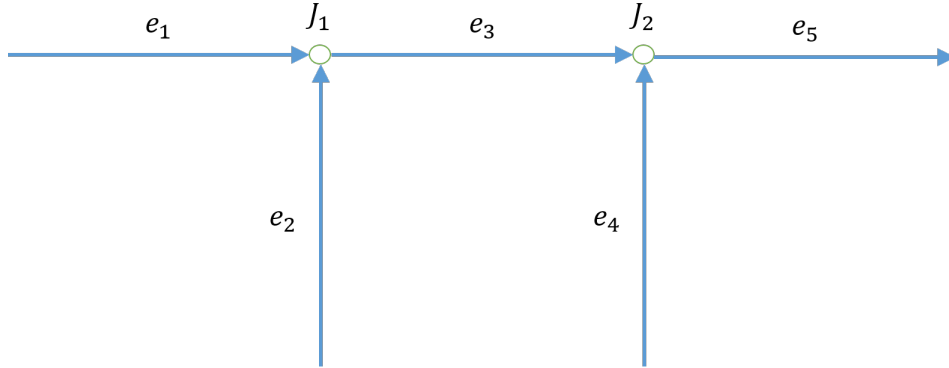
Figure 2.1: Example of a network

Generally for every road e_i we write $\rho_i : [a_i, b_i] \times [0, \infty) \to [0, 1]$ for the density of cars at any point $x \in [a_i, b_i]$ at any time $t \geq 0$. We then want ρ_i to be a weak entropy solution on $[a_i, b_i]$, i.e. for every smooth test function $\phi : [a_i, b_i] \times [0, \infty) \to \mathbb{R}$ with compact support on $(a_i, b_i) \times (0, \infty)$

$$\int_0^\infty \int_{a_i}^{b_i} \left(\rho_i \frac{\delta\phi}{\delta t} + f(\rho_i)\frac{\delta\phi}{\delta x} \right) dxdt = 0 \tag{2.2.1}$$

Definition 2.2.3 *Let J be a junction with n incoming roads and m outgoing roads. A weak solution at J is a collection of functions $\rho_i : [a_i, b_i] \times [0, \infty) \to [0, 1], i = 1, \ldots, n+m$, such that*

$$\sum_{i=1}^{n+m} \left(\int_0^\infty \int_{a_i}^{b_i} \left(\rho_i \frac{\delta\phi_i}{\delta t} + f(\rho_i)\frac{\delta\phi_i}{\delta x} \right) dxdt \right) = 0 \tag{2.2.2}$$

for smooth functions $\phi_i, i = 1, \ldots, n+m$. In particular ϕ is also smooth across junctions, namely

$$\phi_i(b_i, \cdot) = \phi_j(a_j, \cdot), \qquad \frac{\delta\phi_i}{\delta x}(b_i, \cdot) = \frac{\delta\phi_j}{\delta x}(a_j, \cdot)$$

From Definition 2.2.3 we can also follow the so-called Rankine-Hugoniot condition.

Lemma 2.2.4 *Rankine-Hugoniot condition*
Let $\rho = (\rho_1, \cdots, \rho_{n+m})$ be a weak solution at junction J. Then ρ satisfies the Rankine-Hugoniot condition

$$\sum_{i=1}^n f(\rho_i(b_i, t)) = \sum_{j=1}^m f(\rho_j(a_j, t)) \tag{2.2.3}$$

2.3 The Riemann problem

2.4 Modelling of junctions - the buffer model

The setting:

Consider a family of $n + m$ roads, all joining at a single junction. The indices $i \in \{1, ..., m\} =: \mathcal{I}$ hereby denote *incoming roads* and indices $j \in \{m + 1, ..., m + n\} =: \mathcal{O}$ denote *outgoing roads*. Then the evolution of the density of cars $\rho_k(x, t)$ on the $k - th$ road can be described by the **conservation law**

$$(\rho_k)_t + f(\rho_k)_x = 0. \tag{2.4.1a}$$

accompanied by intial densities $\rho_k(x, 0) = \rho_{k,0}(x)$ and external inflows $f(\rho_{in,k})$ into the network defined by

$$f(\rho_k(a_k, t) = f(\rho_{in,k}(t)) \quad \forall e_k \in \mathcal{E}^{in} \tag{2.4.1b}$$

where $\rho_{in,k}(t)$ denotes the incoming densite into road $e_k \in \mathcal{E}^{in}$. Furthermore the corresponding inflows and outflows of the junctions are given as

$$f(\rho_k(b_k, t)) = \bar{f}_k(t) \quad \forall e_k \in \mathcal{E} \setminus \mathcal{E}^{out} \tag{2.4.1c}$$

$$f(\rho_k(a_k, t)) = \hat{f}_k(t) \quad \forall e_k \in \mathcal{E} \setminus \mathcal{E}^{in} \tag{2.4.1d}$$

where the junctions fluxes $\bar{f}_k$ and $\hat{f}_k$ are defined later in equation (2.4.6).
For the roads leaving the network we also impose Dirichlet boundary conditions.

The model

In order to be useful for the analysis of global optimization, the used traffic flow model at junctions should provide two crucial properties:

- Well posedness for $\mathcal{L}^\infty$ data

- Continuous solution w.r.t. weak convergence

Due to the ill-posedness of the general junction model in [10] for certain input data, we need to come up with a different approach.

In [3] a model is proposed where each intersection in the model includes a **buffer** with limited capacity. The current filling level of the buffer in front of the outgoing road $j \in \mathcal{O}$ may be denoted as the *queue length* $q_j(t)$. The rate of flux at which cars from incoming roads enter the intersection is controlled by the current length of the queues. The outgoing fluxes are governed by the queue length and the personal preference destination of the individual drivers, as well as the maximum permitted fluxes on the designated roads.

The main results of their analysis can be stated as:

I. If the queue lenghts q_j for every outgoing road are given, the initial boundary value problems on each road become decoupled and can be solved individually, first on every incoming road, and secondly on every outgoing road. The densities $\rho_k(t,x)$ on every road $k = 1...m+n$ can then be explicitly computed via a Lax type formula [9].

II. Given the densities, the lenghts q_j of the queues can be determined by balancing the influxes and outfluxes of the intersection. The queue lengths can finally be obtained as a fixpoint of a contractive transformation $q \to \Delta(q)$ where q needs to be Lipschitz continuous.

III. The buffer model is thus well-posed at intersections for general $\mathcal{L}^\infty$ data. It is also shown that the traffic flow model is continous w.r.t. weak convergence.

The interested reader is referred to [3] for the proofs.

Let the general setting be as earlier in this section. Further we include two realistic assumtions for the boundary values at the entrance and exit points of junctions:

i. **Driver's preferences** $\Theta_{i,j}$ define the fraction of cars on road i that want to exit the junction in direction of road j.

$$\Theta_{i,j} \in [0,1]$$

ii. **Relative priorities** η_i **given to incoming roads** e.g. external effects like traffic lights

For every junction J we can define the driver's preferences Θ, i.e. the percentage of drivers going from one incoming to out outgoing road, as followed:

Definition 2.4.1 *Given a junction J with $n := |\delta^{in}(J)|$ incoming roads, say $e_1,...,e_n$, and $m := |\delta^{out}(J)|$ outgoing roads, say $e_{n+1},...,e_{n+m}$. Then the traffic distribution matrix Θ is given by*

$$\Theta = \begin{pmatrix} \Theta n+1,1 & \cdots & \Theta n+1,n \\ \vdots & \ddots & \vdots \\ \Theta n+m,1 & \cdots & \Theta n+m,n \end{pmatrix} \tag{2.4.2}$$

where $0 \leq \Theta_{i,j} \leq 1$ for every $i = 1,...,n$ and $j = n+1,...,n+m$. Furthermore we impose the validity condition

$$\Theta_{i,j} \in [0,1], \qquad \sum_{j \in \delta^{out}(J)} \Theta_{i,j} = 1 \quad \forall i = 1,\ldots,n$$

In general, $\Theta_{i,j} = \Theta_{i,j}(t,x)$ needs not to be necessarily constant, but can be time- and location-dependent. In the following it is assumed that the drivers' preferences are known

in advance and that they do not change their itinerary throughout the network. Then the conservation law reads

$$(\Theta_{i,j}\rho_i)_t + [\rho_i\Theta_{i,j}v(\rho_i)]_x = 0$$

Using product rule and reordering yields

$$\rho_i[(\Theta_{i,j})_t + v(\rho_i)(\Theta_{i,j})_x] + \Theta_{i,j}[(\rho_i)_t + (\rho_i v(\rho_i))_x] = 0$$

The second term vanishes as the general conservation law still needs to be fulfilled. For zero density on the road this is fulfilled trivially. For $\rho_i \neq 0$ we obtain the passive scalar transport equation along the flux:

$$(\Theta_{i,j})_t + v(\rho_i)(\Theta_{i,j})_x = 0 \tag{2.4.3}$$

A similar approach has been persued by [4]. In their intersection model the capacity of the queues is arbitrarily big. Cars wanting to enter road j but exceeding the maximum outflux of the intersection are instead stored in the queue. As a consequence there is no backward propagation of queues and therefore no emergence of shocks on incoming roads.

The model by [3] extends this model. Consider a single junction and let $M > 0$ be the maximum capacity of the queue. Then the incoming fluxes into the junction depend on the current degree of occupancy of the buffer, which is defined by

$$q = (q_j)_{j\in\mathcal{O}}, \qquad q \in \mathbb{R}^n$$

The Cauchy problem for traffic flow on a network can thus be formulated as

$$\begin{aligned}
(\rho_i)_t + f_i(\rho_i)_x &= 0 \\
(\Theta_{ij})_t + v(\rho_i)(\Theta_{i,j})_x &= 0
\end{aligned}$$

supplemented by suitable initial conditions.

We denote the boundary values at the junction J by

$$\left\{
\begin{array}{rcll}
\bar{\Theta}_{i,j}(t) &:=& \lim_{x\to 0-}\Theta_{i,j} & e_i \in \delta^{in}(J), e_j \in \delta^{out}(J) \\[2mm]
\bar{\rho}_i(t) &:=& \lim_{x\to b_i-}\rho_i(x,t) & e_i \in \delta^{in}(J) \\[2mm]
\hat{\rho}_j(t) &:=& \lim_{x\to a_j+}\rho_j(x,t) & e_j \in \delta^{out}(J) \\[2mm]
\bar{f}_i(t) &:=& f_i(\bar{\rho}_i(t)) = \lim_{x\to b_i-}f_i(\rho_i(x,t)) & e_i \in \delta^{in}(J) \\[2mm]
\hat{f}_j(t) &:=& f_j(\hat{\rho}_j(t)) = \lim_{x\to a_j+}f_j(\rho_j(x,t)) & e_j \in \delta^{out}(J)
\end{array}
\right. \tag{2.4.4}$$

The **maximum fluxes** that can enter and exit the intersection depend on the current filling level on the incoming and outgoing road, respectively. In particular they are given by the following equations.

- Maximum fluxes on incoming roads:

$$\omega_i := \omega_i(\bar{\rho}) = \begin{cases} f(\bar{\rho}) & \bar{\rho} \le \sigma \\ f(\sigma) & \bar{\rho} > \sigma \end{cases}$$

- Maximum fluxes on outgoing roads:

$$\omega_j := \omega_j(\hat{\rho}) = \begin{cases} f(\sigma) & \hat{\rho} \le \sigma \\ f(\hat{\rho}) & \hat{\rho} > \sigma \end{cases}$$

This property ensures that Riemann problems on incoming roads are solved by waves with negative speed, and Riemann problems on outgoing roads are solved by waves with positive speed.

Based on the junctions fluxes, we can also derive the rate of change of the size of the junction buffer. In detail, conservation of mass yields the additional differential equation for the **evolution of the queue size**

$$\dot{q}_j = \sum_{i \in \mathcal{I}} \bar{\Theta}_{i,j} \bar{f}_i - \hat{f}_j \tag{2.4.5}$$

where $\bar{f}_i, \hat{f}_j$ denote the boundary fluxes at the junction.

We are now ready to state two sets of equations regarding the incoming and outgoing junction fluxes depending on the drivers' choices Θ_{ij} and the queue lenghts q_j.

The first model provides a shared buffer of capacity M for every outgoing junction. Incoming cars can cross the intersection governed by the amount of free space left in the queue, regardless of the car's destination. Once within the junction, cars leave at the maximum rate allowed by the outgoing road of their choice.

Single Buffer Junction model (SBJ): Consider a constant $M > 0$, describing the maximum capacity of the junction at any given time, and constants $c_i > 0, i \in \mathcal{I}$ accounting for priorities given to the differnt incoming roads.
We then require that the incoming fluxes $\bar{f}_i$ satisfy

$$\bar{f}_i = \min\left\{\omega_i, c_i(M - \sum_{j \in \mathcal{O}} q_j)\right\}, \qquad i \in \mathcal{I} \tag{2.4.6a}$$

Furthermore, the outgoing fluxes $\hat{f}_j$ should satisfy

$$\hat{f}_j = \begin{cases} \omega_j & q_j > 0 \\ \min\{\omega_j, \sum_{i \in \mathcal{I}} \bar{f}_i \bar{\Theta}_{i,j}\} & q_j = 0 \end{cases} \tag{2.4.6b}$$

As seen, the outgoing fluxes are uniquely defined once the incoming fluxes are known in addition to the current status of the queue.

The second model uses n different buffers, one for every outgoing road. Once having entered the junction, cars are admitted to their desired road of destination depending on the length of the queue in front of the desired road.

Multiple Buffer Junction model (MBJ): Consider constants $M_j > 0, j \in \mathcal{O}$, describing the maximum capacitis of the buffers in front of the n outgoing roads of the junction at any given time, and constants $c_i > 0, i \in \mathcal{I}$ accounting for priorities given to the differnt incoming roads.
We then require that the incoming fluxes $\bar{f}_i$ satisfy

$$\bar{f}_i = \min\{\omega_i, \frac{c_i(M_j - q_j)}{\Theta_{i,j}}, j \in \mathcal{O}\}, \qquad i \in \mathcal{I}$$

Furthermore, the outgoing fluxes $\hat{f}_j$ should satisfy

$$\hat{f}_j = \begin{cases} \omega_j & q_j > 0 \\ \min\{\omega_j, \sum_{i \in \mathcal{I}} \bar{f}_i \bar{\Theta}_{i,j}\} & q_j = 0 \end{cases}$$

Now we can define the full **buffer model** by Bressan et al. [3]

$$\begin{aligned} (\rho_i)_t + f_i(\rho_i)_x &= 0 & , e_i \in \mathcal{E} & \qquad (2.4.7) \\ \dot{q}_j &= \sum_{i \in \mathcal{I}} \bar{\Theta}_{i,j} \bar{f}_i - \bar{f}_j \\ f(\rho_k(a_k, t) &= f(\rho_{in,k}(t)) & \forall e_k \in \mathcal{E}^{in} \\ f(\rho_k(b_k, t)) &= \bar{f}_k(t) & \forall e_k \in \mathcal{E} \setminus \mathcal{E}^{out} \\ f(\rho_k(a_k, t)) &= \hat{f}_k(t) & \forall e_k \in \mathcal{E} \setminus \mathcal{E}^{in} \end{aligned}$$

with external inflows $f(\rho_{in,k}(t))$ and junctions fluxes $\bar{f}_k(t)$ and $\hat{f}_k(t)$ as defined in (2.4.6).
Let $\rho_k(x,t), e_k \in \mathcal{E}$ and $q_j(t), e_j \in \mathcal{E} \setminus \mathcal{E}^{in}$ now be such that equations 2.4.6 and (2.4.5) are fulfilled. Then we say that the densities $\rho_k(x,t)$ provide a solution to the Cauchy problem (2.4.7) close to the intersections.[1]

Remark:

In the following we restrict ourselves to the use of the single buffer junction model (SBJ).

Limitations of this approach:

- This approach focuses on maximizing the flux of mass through the junction. A counter-intuitive effect of this approach is the following:

---

[1] wondering if definition of Riemann solver is needed somewhere

Consider a trivial junction at $x = 0$ with one incoming and one outgoing road and initial data $\rho_{in} > \sigma$ and $\rho_{out} = 0$. Then the result won't be continuous at $x = 0$. In particular the outgoing flux will be $f^{max} = f(\sigma)$, hence $\rho(0^+, t) = \sigma$ whereas $\rho(0^-, t) > \sigma$ by assumption.

- The buffer model in general violates the Rankine-Hugoniot condition 2.2.4:

$$\sum_{\substack{e_j \in \delta^{out}(J) \\ J \in \mathcal{N}}} \hat{f}_j = \sum_{\substack{e_j \in \delta^{out}(J) \\ J \in \mathcal{N}}} \sum_{\substack{e_i \in \delta^{in}(J) \\ J \in \mathcal{N}}} \bar{f}_i \Theta_{i,j} - \sum_{\substack{e_j \in \delta^{out}(J) \\ J \in \mathcal{N}}} \dot{q}_j \qquad (2.4.8)$$

$$= \sum_{\substack{e_i \in \delta^{in}(J) \\ J \in \mathcal{N}}} \bar{f}_i - \sum_{\substack{e_j \in \delta^{out}(J) \\ J \in \mathcal{N}}} \dot{q}_j \qquad (2.4.9)$$

as $\sum_{\substack{e_j \in \delta^{out}(J) \\ J \in \mathcal{N}}} \Theta_{i,j} = 1$ for every $i \in \delta^{in}(J), J \in \mathcal{N}$. This does not fulfill the Rankine-Hugoniot condition as long as at least one queue q_j changes its length.

Chapter 3

Numerical approximations

In order to solve conservation laws of the form (1.2.4) we usually assume smooth initial conditions $\rho(x, 0)$. We are naturally interested in the difficulties caused by discontinuities in the solution. Straight-forward numerical methods like the finite difference approximation usually have difficulties near the discontinuity. Consider for instance the scalar (linear) advection equation

$$u_t + Au_x = 0, \quad -\infty < x < \infty, t \geq 0$$
$$u(x, 0) = \begin{cases} 1 & x < 0 \\ 0 & x > 0 \end{cases} \tag{3.0.1}$$

Obviously the analytical solution obtained by the method of characteristics is given by a travelling show wave $u(x, t) = u_0(x - At)$ with wave speed A. ADD Lax Equivalence Theorem?? Unfortunately the finite difference approach is inconsistent, as the finite difference approximation to u_x at the discontinuity $x = 0$ will not approach 0, e.g.

$$u_x \sim \frac{u_0(At + h) - u_0(At - h)}{2h} = \frac{0 - 1}{2h} \to -\infty, \text{ as } h \to 0$$

In particular, the *local truncation error*

$$L_k(0, t) := \frac{1}{k}\left[u(0, t + k) - u(0, t)\right] - a\frac{u_0(At + h) - u_0(At - h)}{2h} \tag{3.0.2}$$

for the finite difference scheme does not vanish for $h, k \to 0$ (see also [15]). A numerical method of **order p** fulfills that $L_k(x, t) = \wr(k^p)$. This means that the finite difference scheme for discontinuous data does neither provide local nor global convergence towards the analytical solution.

For linear systems of the form (3.0.1) a wide variety of convergent numerical methods using adjusted finite difference schemes are given. Some possibilites are stated in Table 3.1. First order method (Upwind, Lax-Friedrich) typically produce a flattened solutions compared to the original solutions, whereas second order methods (Lax-Wendroff and Beam-Warming) give oscillations. These phenomena are displayed in Figure 3.1.

Name	Difference equation	Order
Lax-Friedrich	$u(x, t+k) \;=\; \frac{1}{2}\left(u(x+h,t) + u(x-h,t)\right)$ $\quad\quad\quad\quad\quad -\; \frac{k}{2h}A(u(x+h,t) - u(x-h,t))$	1
Upwind $(A > 0)$	$u(x,t+k) \;=\; u(x,t) - \frac{k}{2h}A(u(x,t) - u(x-h,t))$	1
Lax-Wendroff	$u(x,t+k) \;=\; u(x,t) - \frac{k}{2h}A(u(x+h,t) - u(x-h,t))$ $\quad\quad\quad\quad\quad +\; \frac{k^2}{2h^2}A^2\left(u(x+h,t) - 2u(x,t) + u(x-h,t)\right)$	2
Beam-Warming	$u(x,t+k) \;=\; u(x,t) - \frac{k}{2h}A(3u(xh,t) - 4u(x-h,t)$ $\quad\quad\quad\quad\quad +\; u(x-2h,t)) + \frac{k^2}{2h^2}A^2((u(xh,t)$ $\quad\quad\quad\quad\quad -\; 2u(x-h,t) + u(x-2h,t))$	2

Table 3.1: Finite difference schemes for the linear advection problem (3.0.1).

3.1 The Godunov scheme for nonlinear conservation laws

Finite difference schemes as discussed in the introductive part of this chapter provide *smooth* solutions, even if the initial datum of the conservation law contains discontinuities and jumps. Even to nonlinear problems these PDEs can often be linearized and therefore results from the linear FD methods applied in order to obtain convergence results for nonlinear problems [**?**]. There are several limitations to this approach:
Firstly it is not guaranteed that the obtained numerical solution really converges towards the analytical discontinuous solution (see e.g. Burger's equation). Secondly the modelling of travelling waves, in particular the evolution of traffic jams and shocks often emerge from initial discontinuities discontinuities. Thus a different approach has to be persued.

3.1.1 Theory of conservative numerical schemes

Let us consider the x-t-plane as the operating space. We can discretize this space by choosing a mesh with step size $h := \Delta x$ and time step $k := \Delta t$, $\frac{h}{k} = C > 0$ fixed. In particular the mesh points are given by

$$\begin{aligned} x_j &= jh, & j = \ldots, -1, 0, 1, \ldots \\ t_n &= nk, & n = 0, 1, \ldots \end{aligned}$$
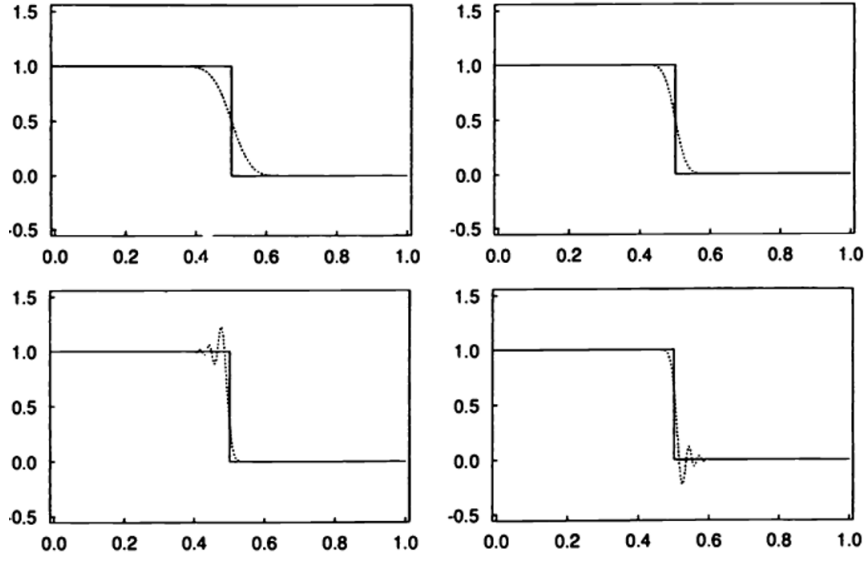
Figure 3.1:   Numerical and exact solution of conservation law (3.0.1) at $t = 0.5$ and step size $h = 0.0025$ using the following methods (top left to bottom right) (a) Lax-Friedrich, (b) Upwind, (c) Lax-Wendroff, (d) Beam-Warming

We also define the midpoints in space

$$x_{j \pm \frac{1}{2}} := x_j \pm \frac{h}{2}$$

We can now define the **cell averages** of the density $\rho(x, t)$ on the mesh as

$$u_j^n := \int_{x_{j-\frac{1}{2}}}^{x_{j+\frac{1}{2}}} \rho(x, t_n) dx \tag{3.1.1}$$

The idea of the **Godunov scheme** is to approximate the solution $\rho(x, t_n)$ to conservation law (1.2.3) by a piecewise constant function

$$u^n(x, t_n) = u_j^n \qquad \text{if } x_{j-\frac{1}{2}} \le x < x_{j+\frac{1}{2}} \tag{3.1.2}$$

and by solving the Riemann problems caused by the space discretization on the time interval $[t_n, t_{n+1}]$. Following from the integral form of conservation law (1.2.3), namely

$$\int_{x_{j-\frac{1}{2}}}^{x_{j+\frac{1}{2}}} \rho(x, t_{n+1}) dx = \int_{x_{j-\frac{1}{2}}}^{x_{j+\frac{1}{2}}} \rho(x, t_n) dx \tag{3.1.3}$$
$$- \left[\int_{t_n}^{t_{n+1}} f(\rho(x_{j+\frac{1}{2}}, t)) dt - \int_{t_n}^{t_{n+1}} f(\rho(x_{j-\frac{1}{2}}, t)) dt \right]$$

we obtain

$$u_j^{n+1} = u_j^n - \frac{1}{h} \left[\int_{t_n}^{t_{n+1}} f(\rho(x_{j+\frac{1}{2}}, t)) dt - \int_{t_n}^{t_{n+1}} f(\rho(x_{j-\frac{1}{2}}, t)) dt \right] \tag{3.1.4}$$

with the **numerical flux function**

$$F(u_j^n, u_{j+1}^n) \sim \frac{1}{k} \int_{t_n}^{t_{n+1}} f(\rho(x_{j+\frac{1}{2}}, t)dt \qquad (3.1.5)$$

which plays the role of the average flux through $x_{j+\frac{1}{2}}$ over the time interval $[t_n, t_{n+1}]$. Numerical methods of the form (3.1.4) are called *in conservative form* as they still fulfill the conservation law.

We also note that in practise equation 3.1.5 simplifies since u_j^n at point $x_{j+\frac{1}{2}}$ is constant along the line $[t_n, t_{n+1}]$ (also see picture ADD picture like LeVeque p.139. Therefore the numerical flux at point $x_{j+\frac{1}{2}}$ only depends on the neighboring densities u_j^n and u_{j+1}^n. Denoting this value by $u^*(u_j^n, u_{j+1}^n$ the numerical flux reduces to

$$F(u_j^n, u_{j+1}^n) = f(u^*(u_j^n, u_{j+1}^n)) \qquad (3.1.6)$$

Obviously the scheme is consistent, since $F(u_j^n, u_j^n) = f(u_j^n))$.
We mentioned earlier that u_j^n at $x_{j+\frac{1}{2}}$ is constant along the line $[t_n, t_{n+1}]$. This only holds if the cells are "small enough" such that two shocks resulting from neighboring Riemann problems do not interact between two time steps. As the wave speed is bounded by the eigenvalue of $f'(u)$ we require that

$$c_C := \frac{k}{h} |\sup(f'(u))| \leq 1 \qquad (3.1.7)$$

c_C is also called the Courant-number and serves as the one-dimensional CFL-condition [7].

The **Godunov method** now consists of seperately solving every Riemann problem between every two neighboring cells. Let u_j and u_{j+1} be the densities on two neighboring cells. Then the flux $f(u^*(u_j, u_{j+1})$ is given by

$$f(u^*(u_j, u_{j+1})) = \begin{cases} \min\left[f(u_j), f(u_{j+1})\right] & \text{if } u_l \leq u_r \\ \max\left[f(u_j), f(u_{j+1})\right] & \text{if } u_l \geq u_r \end{cases} \qquad (3.1.8)$$

This form of the resulting flux function is valid for any general scalar conservation laws, even for nonconvex fluxes. In the convex case we can distinguish 4 cases for the numerical flux (3.1.8), see Figure 3.2:

1. $f'(u_j), f'(u_{j+1}) \geq 0$: Here the solution consists of a rarefaction wave with $u^*(u_l, u_r) = u_j$.

2. $f'(u_j), f'(u_{j+1}) \leq 0$: The solution consists of a rarefaction wave with $u^*(u_l, u_r) = u_{j+1}$.

3. $f'(u_{j+1}) < 0 \leq f'(u_j)$: Then there is a shock through $x_{j+\frac{1}{2}}$ and

$$u^*(u_j, u_{j+1}) = \begin{cases} u_j & : s \geq 0 \\ u_{j+1} & : s < 0 \end{cases}$$

with the shock speed

$$s = \frac{f(u_{j+1}) - f(u_j)}{u_{j+1} - u_j}$$

4. $f'(u_{j+1}) > 0 \geq f'(u_j)$: In this case we have the so-called transonic rarefaction wave and $u^*(u_j, u_{j+1}) = \sigma$, with $u = \sigma$ the unique point at which $f'(u) = 0$ (cf. (1.2.2)).
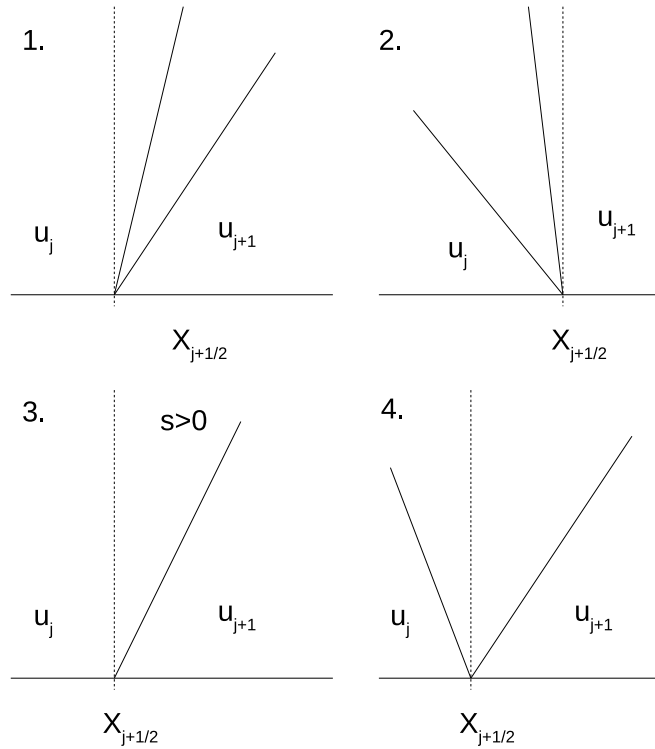

Figure 3.2:   Different types of solutions for the Riemann problem dependent on densities u_j^n and u_{j+1}^n.

In the following we want to apply the Godunov scheme on the buffer model defined in section 2.4.

3.1.2   The Godunov scheme for the buffer model

Let us consider an arbitrary connected road network $(\mathcal{N}, \mathcal{E})$ with n_R roads and n_J junctions. On every road $e_i = [a_i, b_i]$ we apply the discretization $x_{i,j} = a_{i,jh}, j =$

$0, ..., D_i, x_{i,D_i h} = b_i$, with $D_i = \frac{b_i - a_i}{h} - 1$ the number of cells on road e_i. Let us then denote $u_{i,j}^n$ the density on the j-th cell of road e_i at time $t = nk$.

We can now define on all *inner cells* of every road e_i the Godunov scheme

$$u_{i,j}^{n+1} = u_{i,j}^n - \frac{k}{h} \left[f(u^*(u_{i,j}^n, u_{i,j+1}^n)) - f(u^*(u_{i,j-1}^n, u_{i,j}^n)) \right], \qquad e_i \in \mathcal{E}, j = 1, \ldots, D_i - 1$$
(3.1.9a)

We incorporate the *externally inflowing densities* $q_i(t), e_i \in \mathcal{E}^{in}$ by introducing a ghost cell at the beginning of each road e_i. Then we define

$$u_{i,0}^{n+1} = u_{i,0}^n - \frac{k}{h} \left[f(u^*(u_{i,0}^n, u_{i,1}^n)) - f(u^*(v_{i,1}^n, u_{i,0}^n)) \right], \qquad i \in \mathcal{E}^{in}$$
(3.1.9b)

with the inflowing density $v_{i,1}^n := \int_{t_n}^{t_{n+1}} \rho_{in,i}(t)dt$.
The outfluxes leaving the network can be treated analogously.

For junctions we recall equations (2.4.6) for the junction fluxes in the single buffer model. Accordingly, we define for roads coming into junction J

$$u_{i,D_i}^{n+1} = u_{i,D_i}^n - \frac{k}{h} \left[\bar{f}_i - f(u^*(u_{i,D_i-1}^n, u_{i,D_i}^n)) \right], \qquad i \in \delta^{in}(J)$$
(3.1.9c)

For outgoing roads of junction J we analogously define the scheme

$$u_{i,0}^{n+1} = u_{i,0}^n - \frac{k}{h} \left[f(u^*(u_{i,0}^n, u_{i,1}^n)) - \hat{f}_i \right], \qquad i \in \delta^{out}(J)$$
(3.1.9d)

<u>Remarks:</u>

- For the computation of the buffer, which is needed for the junction fluxes, we use a simple difference quotient to approximate $\dot{q}$,

$$q_j^{n+1} = q_j^n + k \left[\sum_{i \in \delta^{in}(J)} \bar{\Theta}_{i,j} \bar{f}_i - \bar{f}_j \right], \qquad J \in \mathcal{N}, j \in \delta^{out}(J)$$
(3.1.10)

- For convenience we condense equations (3.1.9)a-d on road e_i to the condensed Godunov scheme

$$u_i^{n+1} = G(u_i^n)$$
(3.1.11)

3.2   Examples

Chapter 4

Traffic light optimization

As discussed in section 2.4 we can model external effects, especially traffic lights, by assigning relative priorities

$$\eta_i \in [0, 1], \qquad e_i \in \mathcal{E} \setminus \mathcal{E}^{out}$$

to roads prior to intersections. These values have the effect that only a fraction of the flux $\bar{f}_i$ as defined in the buffer model can enter the junction and pass it towards outgoing roads. In particular the binary values $\eta_i = 1$ and $\eta_i = 0$ for road e_i correspond to green and red phases, respectively, for the particular incoming road.

For every junction J the **feasibility condition** must hold. It is given by

$$\sum_{e_i \in \delta^{in}(J)} \eta_i(t) = 1 \tag{4.0.1}$$

assuring that cars from only one road can cross the junction at any time t.

This leads to a necessary update of the junction fluxes. In detail we define the **influx under applied traffic control** as

$$\bar{\bar{f}}_k(t, \eta_k) := \min\{\omega_k, c_k(M - \sum_{j \in \mathcal{O}} q_j)\} \cdot \eta_k(t) \tag{4.0.2}$$

The corresponding **outflux under applied traffic control** is given by

$$\hat{\hat{f}}_j(t, \eta) := \begin{cases} \omega_j & q_j > 0 \\ \min\{\omega_j, \sum_{i \in \mathcal{I}} \bar{\bar{f}}_i \bar{\Theta}_{ij}\} & q_j = 0 \end{cases} \tag{4.0.3}$$

For the conservation law

$$
\begin{aligned}
(\rho_k)_t + f(\rho_k)_x &= 0 & \forall e_k \in \mathcal{E} & \tag{4.0.4a} \\
f(\rho_k(b_k, t)) &= \bar{\bar{f}}_k(t) & \forall e_k \in \mathcal{E} \setminus \mathcal{E}^{out} & \tag{4.0.4b} \\
f(\rho_k(a_k, t)) &= \hat{\hat{f}}_k(t) & \forall e_k \in \mathcal{E} \setminus \mathcal{E}^{in} & \tag{4.0.4c}
\end{aligned}
$$

with junction fluxes $\bar{\bar{f}}_k$ and $\hat{\hat{f}}_k$ on a given network $(\mathcal{N}, \mathcal{E})$ the goal is to optimize the flow on every single road and through their intersections. The considered objective function - or also referred to as *cost functional* - can hereby vary depending on the goals of the simulation and the specific definition of the targeted problem. Typical **objective functions** for the optimization are introduced in the following.

a) Mean travel time

From driver's point of view, the key quantity to determine the quality - and therefore the optimal value - of traffic is related to the time needed to reach the desired location. Taking into account the sum of every personal preference hence leads to the definition of the mean arrival time or **mean travel time** (cf. [6]).
Let $x = 0$ be a point on the network. Then the mean travel time needed to read point $x = \bar{x} > 0$ can be described by

$$T(\bar{x}) := \frac{1}{Q_{in}} \int_{t_0}^{\infty} t f(\rho(\bar{x}, t)) dt$$

where $Q_{in} = \int_{t_0}^{t_{end}} q_0(t) dt$ is the acumulated influx $q_0(t)$ into point $x = 0$ on a compact time interval $[t_0, t_{end}]$.

Remarks:

- This approach expects compactly supported inflow into $x = 0$.

- On complex networks drivers can have distinct preference of their respective arrival points and favoured routes. This means that cars, despite also crossing the point $x = 0$, might never reach the reference point $x = \bar{x}$, which complicates the computation of the average travel time between two points on a network.

b) Cumulative traffic flux

From the traffic planner's perspective a more relevant quantity might be the overall flux on the entire network. Therefore the desired goal is to maximize the total number of cars travelling through the network over a certain time interval.
Following equation 4.0.4 we denote by $\bar{f}$ and $\hat{f}$ incoming fluxes into and outgoing fluxes out of junctions, respectively. Then we can formulate the **cumulated traffic flux** on the network during time $t = [t_0, T]$ as

$$F_T(\eta) := \sum_{i \in \mathcal{E}} \int_0^T \int_{a_i}^{b_i} f(\rho_i(x, t)) dx dt + \sum_{i \in \mathcal{E} \backslash \mathcal{E}^{out}} \int_0^T \bar{\bar{f}}_i(t, \eta_i) dt \qquad (4.0.5)$$

$$+ \sum_{j \in \mathcal{E} \backslash \mathcal{E}^{in}} \int_0^T \hat{\hat{f}}_j(t, \eta) dt$$

where $\bar{\bar{f}}$ and $\hat{\hat{f}}$ are as defined as in equations 4.0.2 and 4.0.3 in the buffer model.

Remark:
During the following optimization studies the cumulative traffic flux is the cost functional of choice.

4.1 Traffic light coordination

Optimally tuned traffic lights settings provide a setting where drivers encounter a green wave, in particular a sequence of consecutive green lights. The distinction between synchronized and coordinated traffic lights is important. Synchronized traffic signals all switch at the same time and are hardly used in pratice. On the other hand coordinated signals are controlled by a master controller are set up such that they progress (switch) in sequence in order to generate a green wave for crossing vehicles. ADD weiter ausfÃ¼hren

4.1.1 The model

Consider a sequence of two intersections with two incoming and one outgoing road (cf. figure 4.1) with inflows $q_k(t)$ for $e_k \in \mathcal{E}^{in}$.
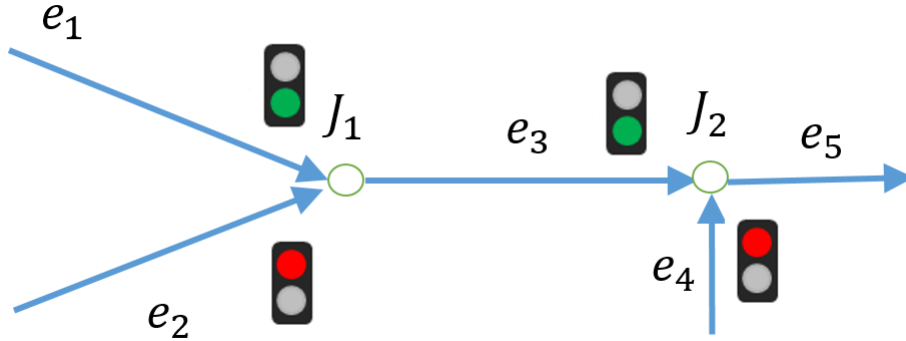
Figure 4.1: Example network consisting of two junctions and four controls.

Then we can refine the conservation law of 1.2.4 to

$$
\begin{align}
(\rho_k)_t + f(\rho_k)_x &= 0 \quad \forall e_k, k = 0, ..., 4 \tag{4.1.1a}\\
f(\rho_k(b_k, t)) &= \bar{\bar{f}}_k(t, \eta_k(t)) \quad \forall e_k, k = 0, 1, 2, 3 \tag{4.1.1b}\\
f(\rho_k(a_k, t)) &= \hat{\hat{f}}_k(t, \eta(t)) \quad \forall e_k, k = 2, 4 \tag{4.1.1c}
\end{align}
$$

accounting the restrictions on the fluxes induced by the traffic configuration η, where $\eta(t) = (\eta_0(t), ..., \eta_3(t)) \in [0, 1]^4$ is the vector containing all control values.

Impose now that the two traffic lights η_0, η_2 have the same fixed frequency of red/green light (also called their lifetime)- say one time unit -, only set apart by a delay τ, and recall the feasibility condition 4.0.1. Then the controls satisfy

$$
\begin{aligned}
\eta_0(t) &= \chi_{[0,1] \cap [2,3] \cap \dots} =: \eta_C(t) \\
\eta_1(t) &= 1 - \eta_C(t) \\
\eta_2(t) &= \eta_C(t - \tau) \\
\eta_3(t) &= 1 - \eta_C(t - \tau)
\end{aligned}
$$

We fix $\eta_C(t)$. The goal now is to find the optimal delay τ in order to obtain the best value for F_T.

In particular, the optimization problem can be formulated as

$$
F_T^* := \max_{\tau \in \mathbb{R}} \quad \sum_{i \in \mathcal{E}} \int_0^T \int_{a_i}^{b_i} f(\rho_i(x,t)) dx dt + \sum_{i \in \mathcal{E} \setminus \mathcal{E}^{out}} \int_0^T \bar{\bar{f}}_i(t, \eta_i(t)) dt
$$

$$
+ \sum_{j \in \mathcal{E} \setminus \mathcal{E}^{in}} \int_0^T \hat{\hat{f}}_j(t, \eta(t)) dt \tag{4.1.2}
$$

and the optimal delay is given by

$$
\tau^* := \quad \arg\max_{\tau \in \mathbb{R}} \sum_{i \in \mathcal{E}} \int_0^T \int_{a_i}^{b_i} f(\rho_i(x,t)) dx dt + \sum_{i \in \mathcal{E} \setminus \mathcal{E}^{out}} \int_0^T \bar{\bar{f}}_i(t, \eta_i(t)) dt
$$

$$
+ \sum_{j \in \mathcal{E} \setminus \mathcal{E}^{in}} \int_0^T \hat{\hat{f}}_j(t, \eta) dt \tag{4.1.3}
$$

4.1.2 Experiments on coordinated light signals

Experiment a)
In the first study we want to examine the effect of the duration of the green and red phases on the total flux on the network. Here we consider a single junction with two incoming roads and one outgoing road, hence the traffic distribution matrix is given by

$$
\Theta = \begin{pmatrix} 0 & 0 & 0 \\ 0 & 0 & 0 \\ 1 & 1 & 0 \end{pmatrix}
$$

Every road is filled initially with traffic density $\rho_i(x, 0) = 0.2, i = 0, 1, 2$. On the incoming roads e_0, e_1 traffic of density $\rho_{in,0} = 0.4, \rho_{in,1} = 0.2$ is constantly inflowing. Cars at the end of road e_2 just exit the network and vanish. The traffic lights η_0, η_1 at the end of the incoming roads switch during time. The period, consisting of one green and red phase cicle, is fixed at $T_s = 50s$. The goal of this experiment is to find the optimal distribution of green times for both light signals based on the densities on the incoming roads. Using compactly supported inflow on both incoming roads in $[0s, 200s]$ we compute the total

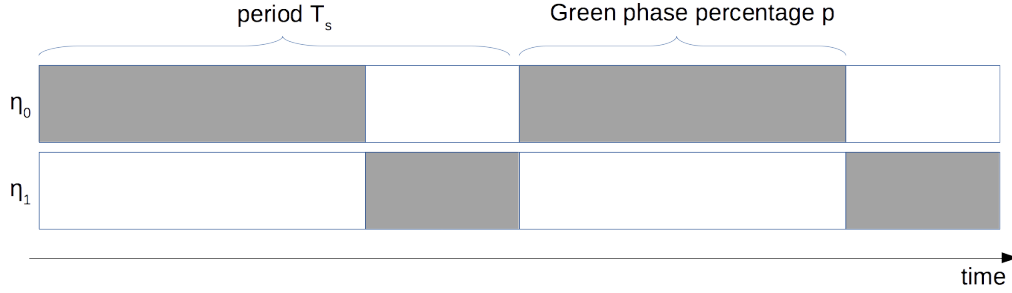| road	length	initial density ρ_0	inflow $f(\rho_{in,i}(t))$ on $[0, 200]$
e_0	50	0.2	f(0.4)
e_1	50	0.2	f(0.2)
e_2	100	0.2	-

Table 4.1: Setup for the network of example a)

Figure 4.2: Switching traffic lights over time.

flux F_T on the network upt to $T = 500s$ for varying green time percentages p_0 (Note, that $p_1 = 1 - p_0$ as it is a valid configuration). The optimal flux is eventually attained if $\eta_0 = 1$ (meaning keeping its green phase) during 56% of its period (cf. Figure 4.3). We then obtain an optimal flux of $F_T \sim 39382.84$.
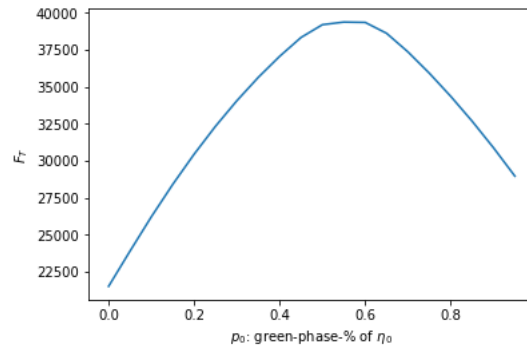
Figure 4.3: Total fluxes on the network dependent on the green time distribution p_0. The optimal flux is obtained if the green phase lasts 0.56 T_s.

Experiment b)

Consider the same network as provided in figure 4.1, hence its traffic distribution matrix is given by

$$\Theta = \begin{pmatrix} 0 & 0 & 0 & 0 & 0 \\ 0 & 0 & 0 & 0 & 0 \\ 1 & 1 & 0 & 0 & 0 \\ 0 & 0 & 0 & 0 & 0 \\ 0 & 0 & 1 & 1 & 0 \end{pmatrix}$$

Also we consider the initial setup given in Table 4.1.2.

road	length	initial density ρ_0	inflow $f(\rho_{in,i}(t))$ on $[0, 200]$
e_0	50	0.2	f(0.4)
e_1	50	0.2	f(0.2)
e_2	100	0.2	-
e_3	50	0.2	f(0.2)
e_4	50	0.2	-

Table 4.2: Setup for the network of example b)

Furthermore let the external inflows be constant over a compact interval $[0s, 200s]$ and let the fixed green/red phase duration be set to 60s. Then the evaluation of our cost functional with respect to the delay $\tau \in [0, 120]$ up to final time $T = 500$, according to equation 4.1.2, leads to an optimal delay of $\tau^* = 34s$ with an optimal cumulated traffix flux $F_T^* \sim 82851.38$.
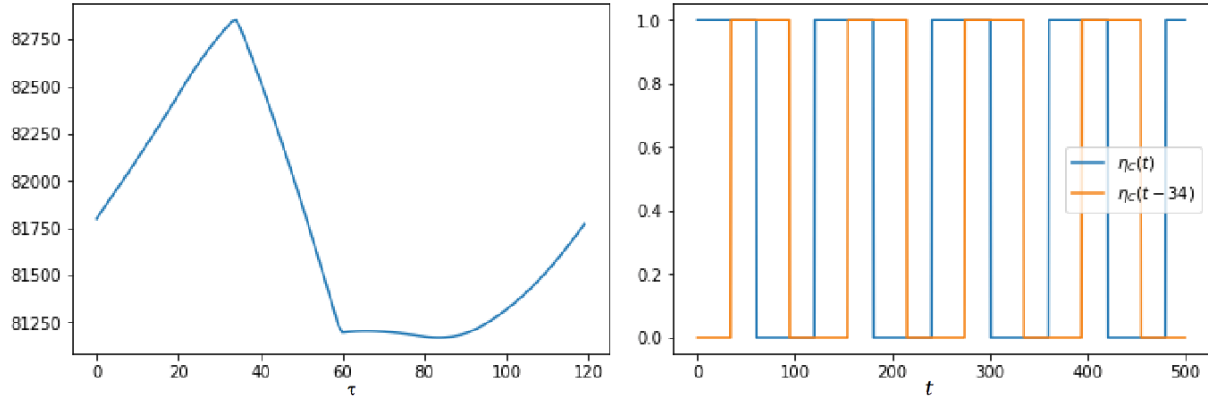
Figure 4.4: Left: Dependency of the cumulated traffix flux F_T on the value for the delay. In experiment b) the objective function attains its maximum $F_T^* = 82851.38$ at $\tau^* \sim 34$. Right: Plotted controls with applied optimal delay τ^*.

TODO:

- Discussion

4.2   Optimization via Model Predictive Control

In contrary to chapter 4.1 the optimal master controller should not work on fixed green and red light periods but be able to adjust traffic lights based on the current - and ideally even future - traffic situation in front of the traffic lights. Based on the possible fluxes the master controller would assign traffic light configurations such that the total flow on the network is maximized over the full time horizon. While trying optimization over the full time horizon we run into two problems:

- In real networks complete knowledge of the future volume of traffic over the whole time horizon is usually not given (at best educated guesses about the volume of traffic and the occupation of the network can be made at certain times throughout the day).

- The computational needed to find the optimal solution might be too high to solve the optimization problem in reasonable time.

This is where **model predictive control** comes into play.

Model Predictive Control (MPC) is a method to control complex dynamic processes and has a wide range of applications. MPC algorithms use a model of the underlying system under consideration in order to find optimal control signals, taking the future behaviour of the system into account. MPC methods are suitable to control systems in which prediction is a key aspect.
The main advantage of MPC over non-predictive control is, that MPC methods inherently make a trade-off between immediate performance and future outputs [12].

MPC is based on an iterative, finite-horizon optimization of an objective function whose state variables are derived from the solution of a system of PDEs.
The finite time interval used for MPC optimization is called **predictive horizon** n_p. The resulting optimal control sequence obtained after one optimization step is then applied as input for the light signals up to a **control horizon** n_c, when the optimization step repeats on the new time interval (Note that the condition $n_c \leq n_p$ needs to be fulfilled). As the predictive horizon keeps being shifted forward MPC is also referred to as *receding horizon control.*

In the following we provide a high level description of the MPC method [13]:

1. **Prediction.** The current state $x(t_n)$ of the system, expected external influences and a planned control signal are used to predict the behavior of the considered system in the the predictive horizon $[t_n, t_n + n_P \Delta t]$. For traffic flow, this involves the evaluation of a model to predict the future road conditions.

2. **Performance evaluation.** An objective function is used to evaluate the performanceof the system under the planned control signal from the prediction phase.

Typical functionals consist of the average travel time or the cummulated traffic flux on the network.

3. **Optimization.** In an optimization step, the optimal control signal is found. This control signal optimizes the objective function for the chosen time horizon of the prediction phase. Typical methods for this step use gradient-descent methods, LP solvers or least-squared methods.

4. **Model dynamics.** Given the optimal control signal from the previous step, the next control action is taken from the optimal control signal and subsequently applied to the system on the control horizon $[t_n, t_n + n_C \Delta t]$. Recalculating optimal control signals proceeds using a receeding horizon scheme.
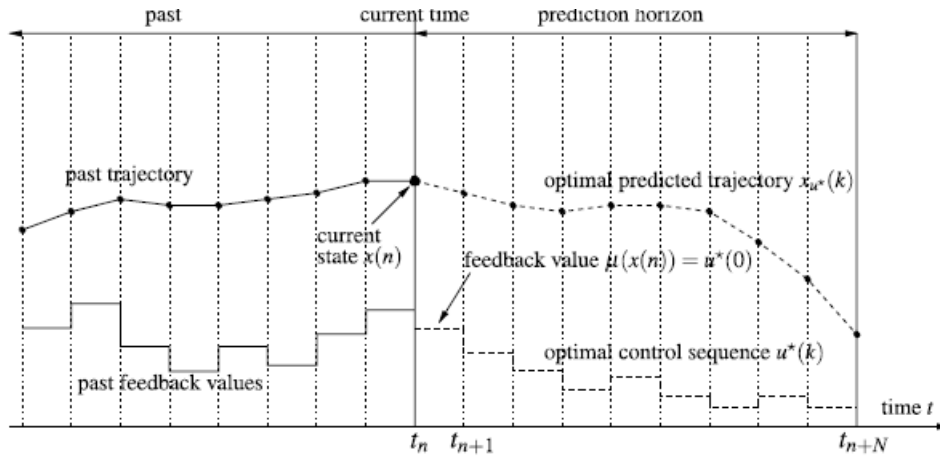
Figure 4.5: Illustration of an MPC step at time t_n ADD better picture

In the following the theory on MPC will be provided, supplemented by numerical examples. Also a comparison with the results from the delay modelling in 4.1 will be given.

4.2.1   Theory

relaxation of binary values for the light signals on $[0, 1]$.

Let $K_i \in \{0,1\}^{n_J}$ be a feasible discrete configuration for all traffic lights such that the feasibility condition 4.0.1 is met, where $K_i^j \in \{0,1\}$ denotes the individual configuration of the $j-th$ traffic light. Then we can define $\Omega := \{K_1, ..., K_{n_\Omega}\}$ as the set of all **feasible discrete traffic light configurations**. ADD different repr of K

Example 2 *For a single junction with 3 incoming and a single outgoing road Ω would be defined in a straight forward way as*

$$\Omega := \left\{ \begin{pmatrix} 1 \\ 0 \\ 0 \end{pmatrix}, \begin{pmatrix} 0 \\ 1 \\ 0 \end{pmatrix}, \begin{pmatrix} 0 \\ 0 \\ 1 \end{pmatrix} \right\},$$

supposing that only one signal can be green at every instant.

The flux functional F_{MPC} over the time interval $[t_n, t_{n+n_c}]$ can then be defined as

$$
\begin{aligned}
F_{MPC}(t_n, \eta) \; := \; & \sum_{i \in \mathcal{E}} \int_{t_n}^{t_n + n_p \Delta t} \int_{a_i}^{b_i} f(\rho_i(x,t)) dx dt + \sum_{i \in \mathcal{E} \backslash \mathcal{E}^{out}} \int_{t_n}^{t_n + n_p \Delta t} \bar{\bar{f}}_i(t, \eta_i) dt \\
+ \; & \sum_{j \in \mathcal{E} \backslash \mathcal{E}^{in}} \int_{t_n}^{t_n + n_p \Delta t} \hat{\hat{f}}_j(t, \eta) dt - \gamma_1 \int_{t_n}^{t_n + n_p \Delta t} \sum_{i=1}^{n_J} W_i(t, \eta_i) dt \\
- \; & \gamma_2 \int_{t_n}^{t_n + n_p \Delta t} ||\dot{\eta}||^2 dt \\
= \; & F_{n_C}(t_n, \eta) - R(t_n, \eta)
\end{aligned}
$$

with $\gamma_1, \gamma_2 > 0$ and where

- $F_{n_C}(t_n, \eta)$ is the target functional refering to the cummulated flux travelled through the network during $t \in [t_n, t_n + n_C \Delta t]$ and

- R marks the penalization terms

  a) $W_i(t) := || \prod_j (\eta_i(t) - K_i^j) ||^2$ is a **multi-well function**, as it is also used in the Modica-Mortola-functional [19]. It works as a de-relaxation term meaning that the resulting controls η_i stay close to the binary values 0 and 1

  b) and the term $||\dot{\eta}||^2$ which limits the frequency with which traffic lights can switch.

Then by substituting the time integrals by finite sums and discretizing the derivative via the backward difference quotient

$$
\int_{t_n}^{t_n + n_p \Delta t} ||\dot{\eta}||^2 dt \sim \gamma_2 \sum_{j=n+1}^{n+n_p} \sum_{i=1}^{n_J} (\eta_i(t_j) - \eta_i(t_{j-1}))^2
$$

we can define the **discrete optimal control problem** (OCP) over the finite horizon $[t_n, t_n + n_p \Delta t]$ as

The resulting flux $F_{n_C}(t_{n \cdot n_C}, u^*)$ is then (locally) optimal on the interval $[t_n, t_n + n_C \Delta t]$. The **total flux** on the network over the entire time horizon $[0, T]$ can finally be computed by summing up the local optima, i.e.

$$
F_{MPC,T}(u^*) = \sum_{n=0}^{n_{MPC}} F_{n_C}(t_{n \cdot n_C}, u^*|_{n_C}(t_n)) \tag{4.2.2}
$$

where n_{MPC} denotes the number of MPC-steps computed.

OCP

$$F_{n_C}(t_{n \cdot n_C}, u^*) := \max_{\eta_i \in [0,1]} F_{MPC,discrete}(t_n, \eta) \tag{4.2.1a}$$

s.t.

valid TL configs	$\sum_{e_i \in \delta^{in}(J)} \eta_i(t_k) = 1, \quad k = n...n + n_p, J \in \mathcal{N}$	(4.2.1b)
Godunov scheme	$\rho^{n+1} = G(\rho^n, \eta(t_n))$	(4.2.1c)
maximum fluxes	$\omega_i, \omega_j, \text{cf.2.4}$	(4.2.1d)
junction influxes	$\bar{\bar{f}}_i = \min\{\omega_i, c_i(M - \sum_{j \in \mathcal{O}} q_j)\}$	(4.2.1e)

$$\text{junction outfluxes} \quad \hat{\bar{f}}_j = \begin{cases} \omega_j & q_j > 0 \\ \min\{\omega_j, \sum_{i \in \mathcal{I}} \hat{\bar{f}}_i \bar{\Theta}_{ij}\} & q_j = 0 \end{cases} \tag{4.2.1f}$$

queue	$q_j^{n+1} = q_j^n + \Delta t \left(\sum_{i \in \mathcal{I}} \bar{\Theta}_{ij} \bar{\bar{f}}_i - \bar{\bar{f}}_j \right)$	(4.2.1g)
inital values	ρ_i^n, q_j^n, η^n	(4.2.1h)
external inflow	$\rho_i(0, t_m) \forall m = 0, 1...n_T \forall i \in \mathcal{E}^{in}$	(4.2.1i)

Figure 4.6: The MPC optimal control problem.

A similar variation of algorithm 1 can be found in [11]. The solution of this algorithm then converges to a local optimum and for appropriate choices of γ_1, γ_2 the elements of the optimal control sequences are close to binary.

Justification of the use of $W(t)$ and $||\dot{\eta}||$:

Consider a simple network consisting of a single junction with two incoming roads and one outgoing road. Initially the network is empty, so $\rho_i(x, 0) = 0 \forall i = 1...3$. In the given network we have two traffic lights (controls) η_1 and η_2 referring two the two incoming roads. Furthermore at every time step t the feasibility condition 4.0.1 is satisfied.
Using this basic network we want to evaluate the effect of the two additional terms $W(t)$ and $||\dot{\eta}||$.

Algorithm 1 *(MPC)*
For every sampling time $t_n, n = 0, n_c, 2n_c...$ do the following steps 1.-4.:

1. Measure the densities $\rho_i(x, t_n)$ on every road e_i of the network

2. Solve the OCP 4.2.1 and denote the resulting optimal control sequence for TL i by $\eta_i^* := \{\eta_i(t_n), \eta_i(t_{n+1}), ..., \eta_i(t_{n+n_p})\}$

3. Apply the quantization function

$$Q(\eta) := \begin{cases} 1 & \eta \geq 0.5 \\ 0 & \eta < 0.5 \end{cases} \tag{4.2.3}$$

   on the optimal control sequence $u_i^*|_{n_c} := \{\eta_i(t_n), \eta_i(t_{n+1}), ..., \eta_i(t_{n+n_c})\}$ in order to obtain a (sub-)optimal binary control sequence $u_{i,bin}^*|_{n_c}$.

4. Take $u_{bin}^*|_{n_c} := \{u_{0,bin}^*|_{n_c}, u_{1,bin}^*|_{n_c}, ..., u_{n_J,bin}^*|_{n_c}\}$ as an input for the Godunov scheme to obtain densities $\rho_i(x, t_{n+n_c})$ and to compute the (sub-)optimal flux $F_{n_C}(t_n, u_{bin}^*|_{n_c})$. Proceed with 1.

5. Compute the total flux $F_T(u_{bin}^*)$ based on equation 4.2.2.

Figure 4.7: The MPC algorithm.

	fluxes	computation time $[s]$
a)	48517.24	518.28
b)	48120.96	417.30
c)	48503.42	295.84
d)	48398.24	396.31

Table 4.3: Resulting optimal fluxes and needed computation time for the different functionals
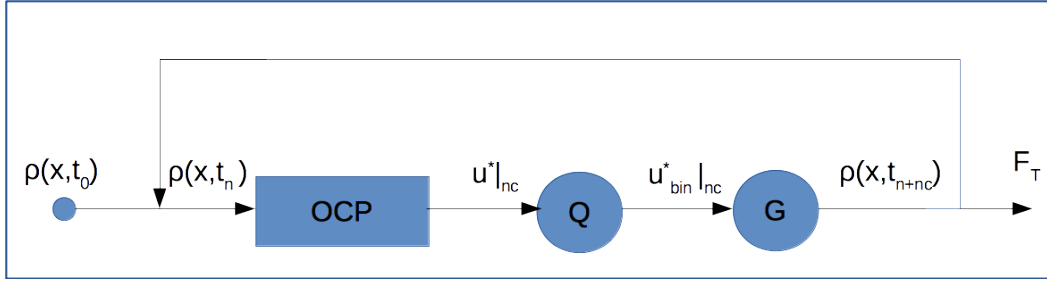
Figure 4.8: Closed loop diagram of the MPC algorithm.

4.2.2   Numerical experiments

To solve the optimization problems (4.2.1) we use a sequential least squares programming optimizer (SLSQP) implemented as part of the SciPy module[1] in Python 2.7[2]. The SLSQP uses the Han-Powell quasi-Newton method with a Broyden-Fletcher-Goldfarb-Shanno (BFGS) update [14]. In particular we choose the convergence accuracy $\epsilon = 10^{-6}$ for the optimization. All simulations were performed on a 8 GB DDR3 RAM Apple MacBook Pro with a 2,6 GHz Intel Core i7 processor.

a) Evaluation of the MPC algorithm:
First we evaluate the computational cost and overall performance of the MPC algorithm. Therefore we use a simple junction consisting of two incoming incoming roads (as in section 4.1.2 Experiment a)) and compare the different results which are given in Table 4.4.

Table 4.4:   Optimal flux F_T and total computational cost in $[s]$ (in brackets) for different choices for the predictive horizon n_p and the control horizon n_c.maybe add 3D plot?

n_c	1	5	10	20
			n_p	
1	29036 (40)	38635 (334)	39388 (2073)	39390 ($\sim 1d$)
5		39384 (114)	39389 (559)	39390 ($\sim$4h)
10			39408 (322)	39390 (3225)
15				39390 (1650)
20				39408 (1491)

Comments:

- The general observation states that the optimal flux increases with increasing the predictive horizon. Nevertheless the size of the control horizon and the compuational

---

[1]Jones E, Oliphant E, Peterson P, et al. SciPy: Open Source Scientific Tools for Python, 2001-, http://www.scipy.org/

[2]Python Software Foundation.   Python Language Reference, version 2.7.   Available at http://www.python.org
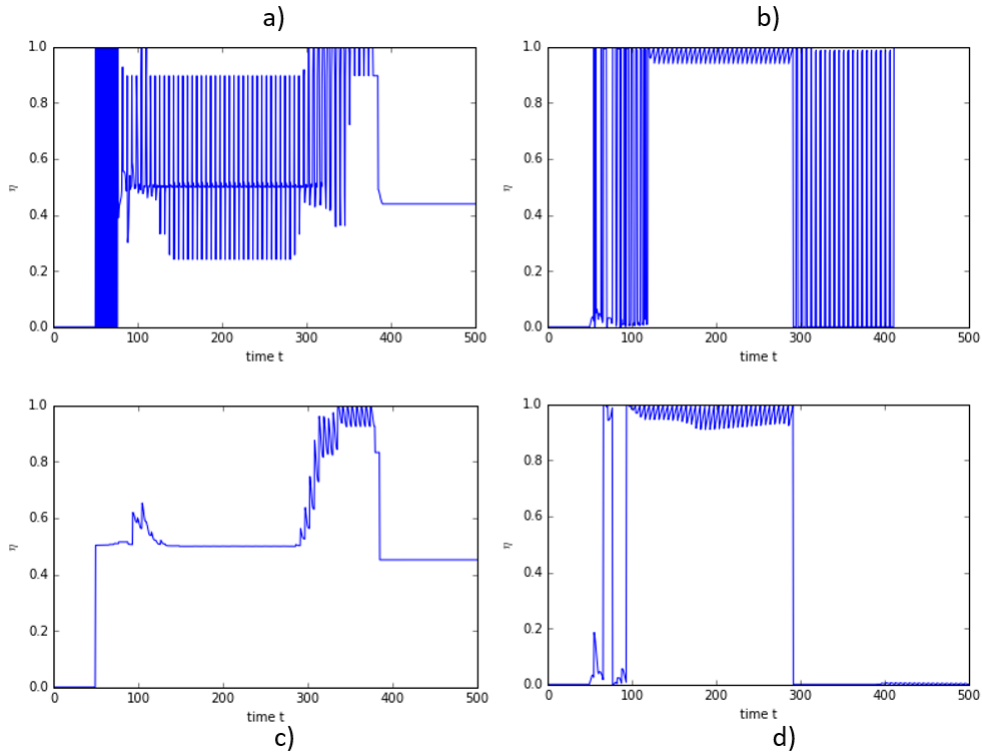
Figure 4.9: Plots of control $\eta_1(t)$ using different functionals. (a) The flux functional $\tilde{F}$ without considering terms $\tilde{W}$ and $\tilde{D}$. We notice high frequencies between 0-(red-)phases and 1-(green-)phases and the existence of clearly non-binary states $\eta_1(t) \in (0,1)$. (b) $\gamma_1 = 0, \gamma_2 = 10$. Application of the de-relaxation term $\tilde{W}$. The rate of occurrance for non-binary controls is reduced. Nevertheless we still observe high frequencies of switching. (c) $\gamma_1 = 10, \gamma_2 = 0$. Application of switching cost $||\dot{\eta}||$. Switching frequencies are decreased but mainly non-binary control states occur. (d) $\gamma_1 = 10, \gamma_2 = 10$. Both de-relaxation and switching cost are applied. Low frequency and mainly binary states occur.

cost are indirect proportional to each other since the OCP has to be performed more often for smaller n_c as the predictive horizon is receeded by a smaller time interval.

- Secondly for very short predictive horizons we see different behavior. In the beginning traffic signals switch rapidly in order to level the different densities on the incoming roads. Nevertheless as one road becomes congested the traffic light misses the incentive to change the signal and therefore might keep its current setting until one road is totally empty. As for this setup the future does not play any or only a minor role, we also refer to it as *instantanous control* (see Figure 4.10 left).

- On the other hand for larger predictive horizons the future dynamics are of more and more importance. We also observe less frequent switches and longer periods (see Figure 4.10 right).
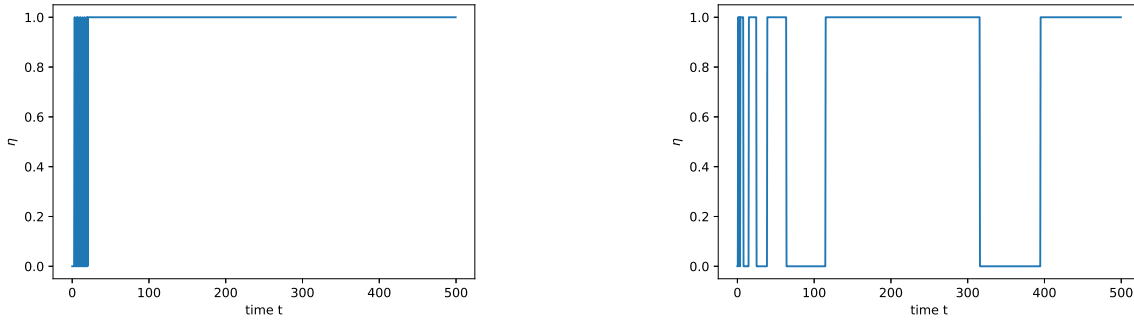
Figure 4.10: Resulting control plots for $\gamma_1 = \gamma_2 = 5$. Left: Control η_0 for $n_c = n_p = 1$. Right: Control η_0 for $n_p = 10, n_c = 1$.

Comparison to the delay model:
With the MPC approach with sufficiently large n_p we obtain similar results for the optimal flux compared to the delay model with optimal green time distribution (Section 4.1.2 Experiment a). Nevertheless the MPC model is a lot more responsive to changes in the incoming fluxes or the general traffic situation on the network. For instance if the inflow on road 1 stops at some point in time, the delay model would still force cars on road 0 to stop and wait, while in the MPC approach the traffic lights would adapt to the current situation and switch to green light for road 0.

b) network with 2 junctions - same as 4.1.2

same input values as in 4.1.2

n_p	n_c	F_T	computation time $[s]$
10	10	89723.626	518.85

comparing this to the optimal delay value in 4.1.2: $F_T(\tau^*) \sim 83174.7$
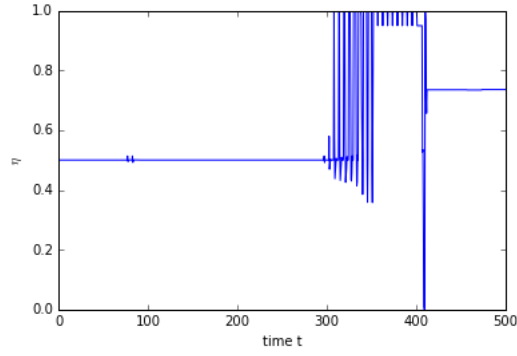
Figure 4.11: abb

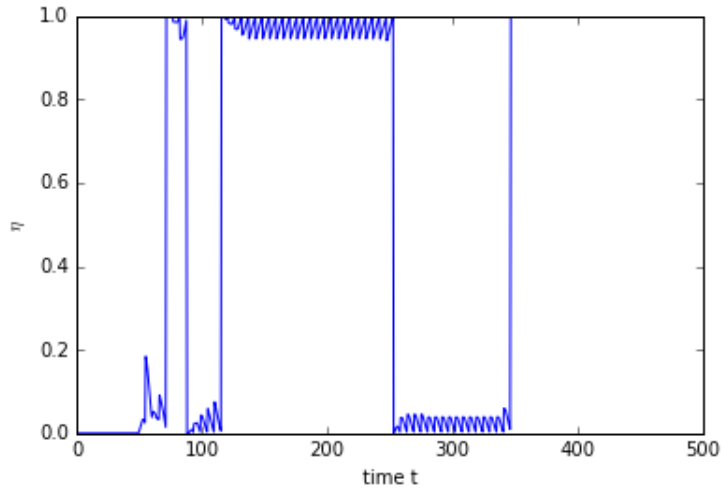c) network with 2 junctions: initially empty

Figure 4.12: Plot of control $\eta_1(t)$ for a 2-junction network with 0 inital data

Chapter 5

Pollution

5.1 Motivation

5.2 The 2D diffusion model

5.2.1 Setting

Let us consider an urban domain $D \in \mathbb{R}^2$ including a road network composed of n_R unidirectional roads that meet at n_J intersections. We impose that the endpoints of each road are either on the boundary of D or connected to one of the junctions. Each road is mapped onto the domain D via

$$
\begin{aligned}
\sigma_i : \quad [a_i, b_i] \quad &\to A_i \subset D \\
s \quad &\mapsto \sigma_i(s) = (x_i(s), y_i(s))
\end{aligned}
\tag{5.2.1}
$$

Here σ_i denotes the parametrization of the segment A_i and mirrors the movement of cars on the road. In particular let $p_i, q_i \in A_i$ be start and end points of the segment A_i and s a point on road e_i. Then we can write the map $\sigma(s)$ as the convex combination of p_i and q_i, namely

$$
\sigma_i(s) = \left(1 - \frac{s - a_i}{b_i - a_i}\right) p_i + \frac{s - a_i}{b_i - a_i} q_i
\tag{5.2.2}
$$

where $\frac{s - a_i}{b_i - a_i} = N(s)$ denotes the normalization of $[a_i, b_i]$ onto $[0, 1]$.

We study the CO transport in a urban area D with a simple two-dimensional transport diffusion model

$$
\frac{\delta \Phi}{\delta t} - \Delta \cdot \mu \Delta \Phi = F(\sigma, t)
\tag{5.2.3a}
$$

where $\Phi(\sigma, t)$ denotes the CO concentration at a point $\sigma = (x, y) \in D$ at the time moment $t \in [0, T]$. $F(\sigma, t)$ describes the CO emission rates based on the solution of the LWR-model (see later......) and Δ is the two-dimensional gradient. $\mu(\sigma, t)$ denotes the diffusion coefficient describing how the particle movement on the domain. In general the coefficients $\mu(\sigma, t)$ are rather complicated functions and difficult to determine. To simplify
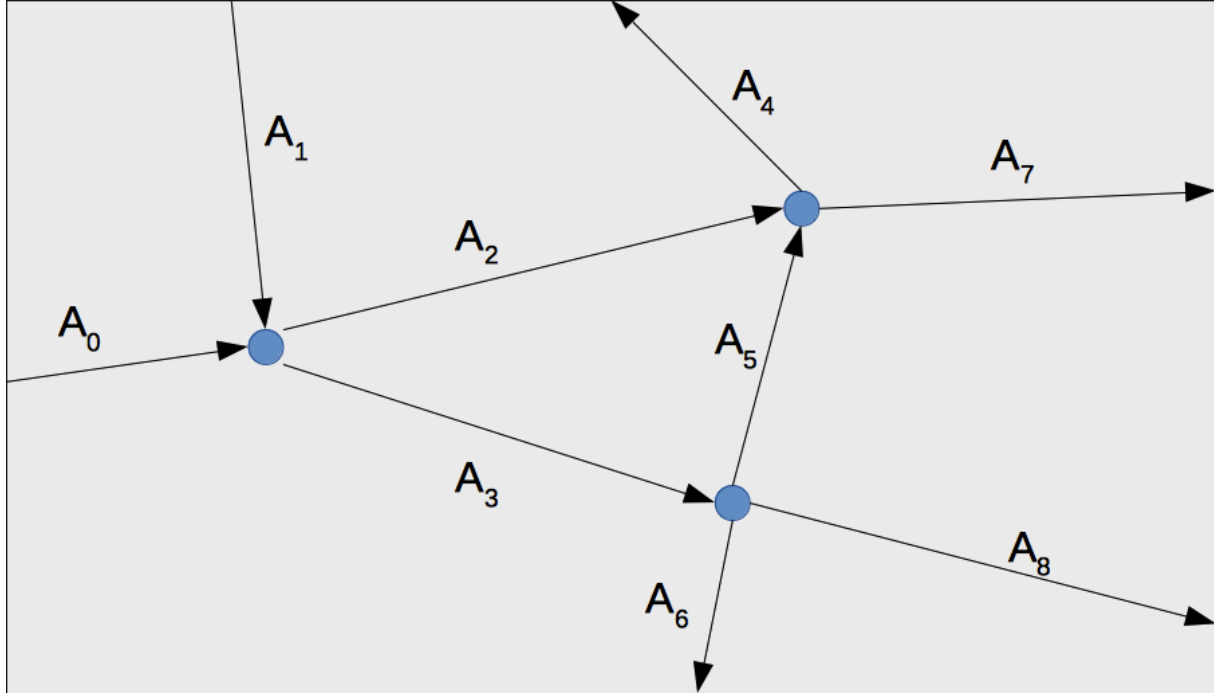
Figure 5.1: Schematic diagram of a 2D domain containing a network of $n_R = 9$ unidirectional roads and $n_J = 3$ junctions.

the problem these functions are approximated by constant values $\mu(\sigma, t) = \mu$.

As initial and boundary conditions we take

$$\phi(r, 0) = \phi_0(\sigma) \qquad \text{at } t = 0 \tag{5.2.3b}$$

$$\mu \frac{\delta}{\delta n} = 0 \qquad \text{on } \delta D \tag{5.2.3c}$$

with δD the boundary of the domain D.

In contrast to ....cite.... this is a simplistic model which only simulates the diffusion of particles emitted by travelling cars. It does not account for advection caused by atmospheric wind or other natural phenomena like interparticle reactions.

As the CO sources we consider vehicular emissions along n_R roads:

$$F(r, t) = \begin{cases} F_i(\sigma, t) & \text{if } \sigma \in A_i \\ 0 & \text{else} \end{cases} \qquad i = 0, \ldots, n_R - 1 \tag{5.2.4}$$

We will assume here that the vehicle emissions are dependent on the velocity and the density of cars on the road, which will be known from the solution of the buffer model

(2.4). In particular we propose to model the source of pollution due to vehicular traffic by:

$$F_i(\sigma, t) = \gamma_i \xi\left(v(\sigma_i(s), t)\right) \rho_i(\sigma_i(s), t) \tag{5.2.5}$$

where γ_i is the contamination rate and $\xi(v)$ for every $t \in [0, T]$ and $\sigma \in A_i$ denotes the velocity dependent fuel consumption rate of a single vehicle on the segment A_i. We impose that $\xi(v)$ is a Lipschitz function in v. A typical representation of ξ can be found in [17?] (see Figure 5.2).
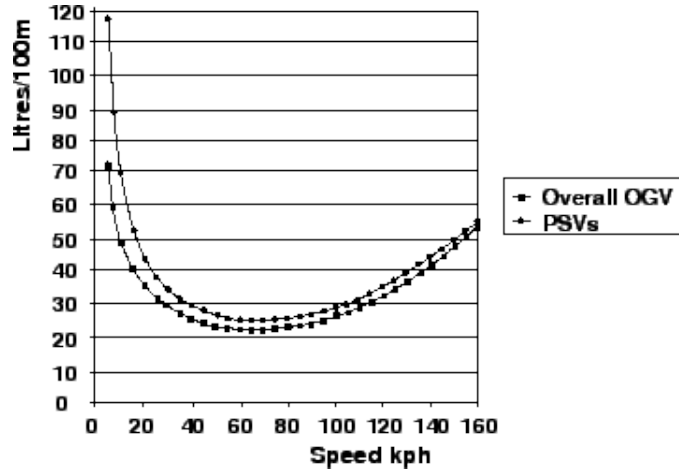
Figure 5.2: Fuel consumption as a function of speed.

For an arbitrary section $[\sigma_i(x), \sigma_i(y)] \subset A_i, x, y \in e_i$ we can then define the cumulated pollution at time t as

$$\int_{\sigma_i(x)}^{\sigma_i(y)} F_i(\sigma, t) d\sigma = \int_x^y \gamma_i \xi(v(s, t)) \rho_i(s, t) ||\sigma'(s)|| ds \tag{5.2.6}$$

Noting that $||\sigma_i'(s)|| = \frac{1}{b_i - a_i} ||p_i - q_i||$ we observe that the lengths of segment $a_i \subset \mathbb{R}^2$ coincide with the length of road e_i whenever $||\sigma_i'(s)|| = 1$.

5.2.2 Analytical solution

From the fact that $\rho_i(x, \cdot) \in L^1_{loc}$ and $\xi(v)$ Lipschitz in v and assuming that $\phi_0 \in L^2()$, we can define weak solutions for problem (5.2.3).

Definition 5.2.1 *Given $r, p \in [1, 2)$ such that $\frac{2}{r} + \frac{2}{p} > 3$. Then we say that a function $\phi \in L^r(W^{1,p}(D); 0, T)$ is a weak solution of problem (5.2.3) if for all testfunctions $v \in$*

$\mathcal{C}^1(\bar{} \times [0, T])$ *with* $v(\cdot, T) = 0$ *the following equality is verified:*

$$\int_0^T \int_D \left(-\int_0^T \int_D \phi(t, \sigma) + mu \nabla \phi \nabla v d\sigma dt \right) = \int_D \phi(x, 0) v(x, 0) dx$$

$$+ \sum_{i=0}^{n_R} \int_{a_i}^{b_i} \gamma_i \xi(v(\rho_i(s, t))) \rho_i(s, t) ||\sigma'(s)|| ds$$

Now we can prove the following existence and uniqueness result:

Theorem 5.2.1 *abb*

Chapter 6

Conclusion and possible extensions

- Instead of MPC one could use compass search in order to determine the time points at which traffic lights switch...ref to handwritten papers

Abbreviations

LWR	Lighthill-Whitham-Richards
MPC	model predictive control
ODE	ordinary differential equation
OCP	optimal control problem
PDE	partial differential equation
TL	traffic light

List of Figures

Bibliography

[1] A. Aw and M. Rascle. Resurrection of second order models of traffic flow. *SIAM Journal on Applied Mathematics*, 60(3):916–938, 2000.

[2] N. L. Biggs. *Algebraic graph theory*. Cambridge mathematical library. Cambridge Univ. Press, Cambridge, 2. ed. edition, 1993.

[3] A. Bressan. Conservation law models for traffic flow on a network. 2014.

[4] A. Bressan and K. Han. Existence of optima and equilibria for traffic flow on networks. *Networks and Heterogeneous Media*, 8(3):627–648, 2013.

[5] D. J. Buckley. A semi-poisson model of traffic flow. *Transportation science : the publication of the Transportation Science Section, Operation Research Society of America*, 2 (1968):107–133, 1968.

[6] R. M. Colombo, P. Goatin, and M. D. Rosini. On the modelling and management of traffic. *ESAIM: Mathematical Modelling and Numerical Analysis*, 45(5):853–872, 009 2011.

[7] R. Courant, K. Friedrichs, and H. Lewy. Über die partiellen differenzengleichungen der mathematischen physik. *Mathematische Annalen*, 100(1):32–74, 1928.

[8] S. S. E. Cristiani. On the micro-ta-macro limit for first-order traffic flow models on networks. *arXiv:1505.01372 [math.DS]*, 2015.

[9] L. C. Evans. *Partial differential equations*, volume Volume 19 of *Graduate studies in mathematics*. American Mathematical Society, Providence, Rhode Island, second edition, reprinted with corrections edition, 2015.

[10] M. Garavello and B. Piccoli. *Traffic flow on networks: Conservation laws model*, volume v. 1 of *AIMS series on applied mathematics*. American Institute of Mathematical Sciences, Springfield, MO, 2006.

[11] L. Grüne and J. Pannek. *Nonlinear model predictive control: Theory and algorithms*. Communications and Control Engineering. Springer, Cham, Switzerland, second edition edition, 2017.

[12] A. Hegyi. *Model Predictive Control for Integrating Traffic Control Measures.* PhD thesis, Technische Universiteit Delft, 2004.

[13] S. Hein. *MPC/LQG-Based Optimal Control of Nonlinear Parabolic PDEs.* PhD thesis, TU Chemnitz, 2009.

[14] D. Kraft. *A software package for sequential quadratic programming*, volume 88-28 of *Forschungsbericht / Deutsche Forschungs- und Versuchsanstalt für Luft- und Raumfahrt.* DFVLR, Köln, als ms. gedr edition, 1988.

[15] R. J. LeVeque. *Numerical methods for conservation laws.* Lectures in mathematics. Birkhäuser, Basel, 2. ed. edition, 1992.

[16] R. Mahnke and R. Kühne. Probabilistic description of traffic breakdown. *Traffic and granular flow '05*, pages 527–536, 2007.

[17] T. V. Mathew. Fuel consumption and emission studies. `https://www.civil.iitb.ac.in/tvm/1111_nptel/583_FuelEmi/plain/plain.html`, 2014. Accessed: 2017-03-03.

[18] A. D. May. *Traffic flow fundamentals.* Prentice Hall, Englewood Cliffs, N.J., 1990.

[19] L. Modica and S. Mortola. Il limite nella γ-convergenza di una famiglia di funzionali ellittici. *Boll. Un. Mat. Ital. A (5)*, 14(3):526–529, 1977.

[20] H. J. Payne. *Models of freeway traffic and control.* Simulation Councils, Inc, La Jolla, Calif., 1971.

[21] L. A. Pipes. *An operational analysis of traffic dynamics*, volume no. 25 of *Institute of Transportation and Traffic Engineering.* Institute of Transportation and Traffic Engineering, University of California, [Berkeley, Calif.], 1953.

[22] P. I. Richards. *Shock waves on the highway*, volume 4. 1956.

[23] M. Stachl. Traffic flow optimization on networks. `https://github.com/mstachl/Traffic-flow-thesis`, 2017.

[24] F. Wageningen-Kessels, H. van Lint, K. Vuik, and S. Hoogendoorn. Genealogy of traffic flow models. *EURO Journal on Transportation and Logistics*, 4(4):445–473, 2015.

List of changes